

# Instability of a nematic liquid crystal in a biharmonic electric field

B. I. Lev, V. N. Sergienko, P. M. Tomchuk, and E. K. Frolova

*Institute of Physics, Ukrainian National Academy of Sciences, 252028 Kiev, Ukraine*

(Submitted 8 June 1995)

*Pis'ma Zh. Éksp. Teor. Fiz.* **62**, No. 2, 129–134 (25 July 1995)

New characteristic behavior of a nematic liquid crystal (NLC) under the simultaneous action of electric fields with two different frequencies is reported. The changes in the external parameters gave rise to a series of new phenomena: In the case of close frequencies a great diversity of structures of the spatially periodic distribution of the director, including new structures which “intergrow” and “flicker” with the beat frequency, was recorded. In the case of a large frequency difference the critical field for the appearance of Williams domains depends monotonically on the higher frequency and this dependence saturates. A theoretical explanation of the observed effects is given. © 1995 American Institute of Physics.

1. Electrohydrodynamic instabilities (EHI) in liquid crystals (LCs) have traditionally been investigated in constant or alternating sinusoidal electric fields. Depending on the characteristics of the liquid crystals (anisotropy of the permittivity, conductivity, and viscosity), different structures appear in different frequency ranges: Williams domains, cellular structures, and others. Since the response of a liquid crystal to an external action is nonlinear, it can be expected that the application of an external electric field with a more complicated (than sinusoidal) temporal behavior will lead both to the formation of structures of a new type and to a change in the characteristics of known structures. The simplest case of a more complicated signal is a superposition of two harmonic waves with the same amplitude. In the present paper we report the results of an experimental study of nematic liquid crystals in a biharmonic electric field.

2. A MBBA nematic liquid crystal with a mesophase in the temperature range 21–40 °C was investigated. The crystal was placed in a flat cell with a planar orientation of the director. A sinusoidal voltage with the same amplitude from two generators was applied to the semitransparent electrodes of the hermetically sealed cell. The frequency of one signal was fixed and the frequency of the other signal was varied in the range 20 Hz–100 kHz.

To record the threshold of an instability, we made use of the fact that the structure which is formed has a spatially periodic character. The instability threshold is recorded according to the appearance of a diffraction pattern produced after monochromatic light from a He–Ne laser passes through the liquid-crystal cell. At voltages close to the threshold voltage, initially only one secondary maximum appears on each side of the diffraction pattern (usually the strongest second-order maxima). This indicates the onset of the deformation of the director. This method always makes it possible to record the same

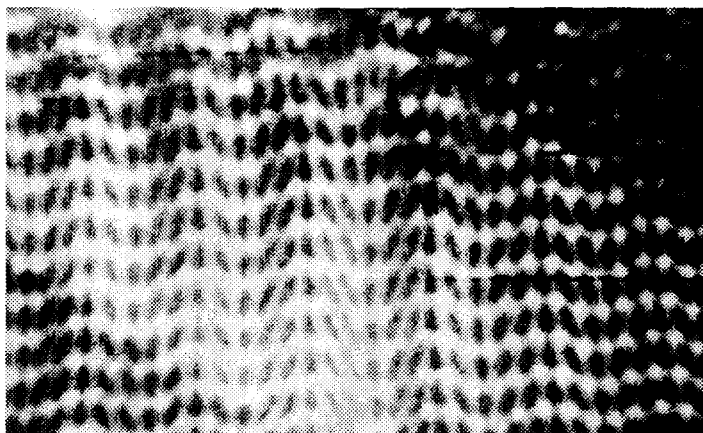


FIG. 1. Picture of the instability of a ZHK-440 liquid crystal. This picture was obtained in a flat cell at room temperature in the beat regime: The carrying frequency was 300 Hz, the beat period was 1 s, and the maximum amplitude was 30 V.

(over a period) deviation of the director with the indicated form of the signals employed.

The experimental apparatus makes it possible to observe the state of the mesophase directly through a polarization microscope and to follow, at the same time, the intertransformations of the possible structures as a function of the applied voltages and ratio of the frequency. We made a video film in which the large diversity of all possible known structures, as well as the appearance of new structures, two of which are shown in Figs. 1 and 2, were recorded. The peculiarities of the behavior of the medium are observed even on the plot of the critical field for the appearance of Williams domains versus the frequencies of the applied voltages.

Figure 3 shows for a 48- $\mu\text{m}$ -thick cell the threshold voltage ( $V_{\text{th}}$ ) of the instability of a uniform distribution of the director as a function of the frequency of the applied

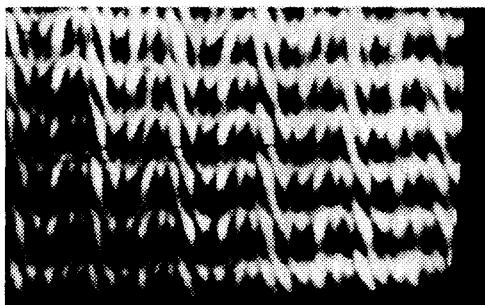


FIG. 2. Picture of the instability of a ZHK-440 liquid crystal. This picture was obtained in a flat cell at room temperature in the beat regime: The carrying frequency was 350 Hz, the beat period was 1.5 s, and the maximum amplitude was 50 V.

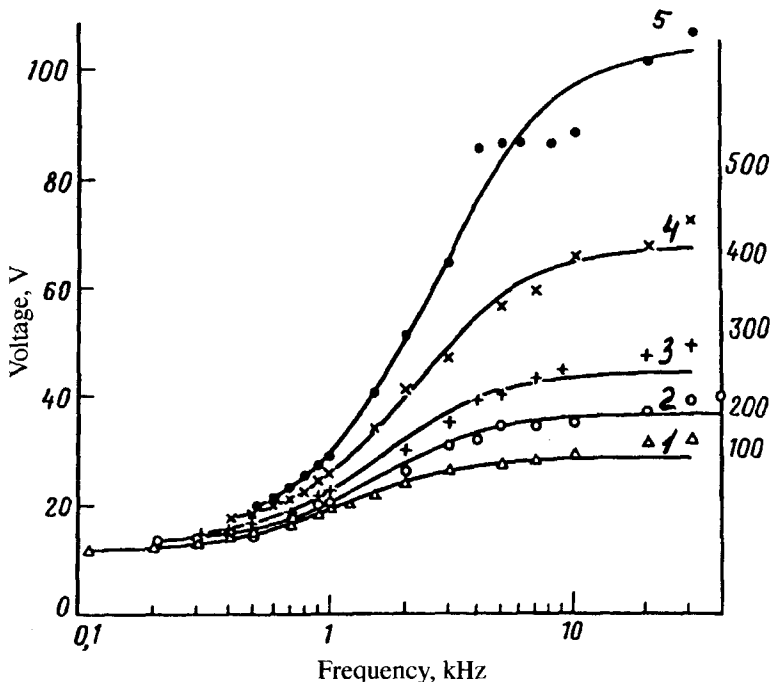


FIG. 3. Voltage  $V_{th}$  at which an instability appears versus the frequency  $f_1$  (Hz) with fixed frequency  $f_2$ : curve 1—100 Hz; 2—200 Hz; 3—300 Hz; 4—400 Hz; 5—500 Hz.

voltage of one of the components of the electric signal with the other frequency held fixed. It should be noted that the threshold field saturates as a function of the high frequency in the case of a large frequency difference and the threshold voltage is minimum when the frequencies are equal to one another.

The behavior of the threshold voltages with a small frequency difference (beats) was investigated in greater detail. The diffraction maxima, according to which the instability threshold was recorded in this region periodically, appear and disappear in time with a frequency equal to the beat frequency. As the voltage increases, the diffraction maxima of the next order appear, just as in all other cases, and the entire diffraction pattern “scintillates.” As the frequency difference increases, the scintillation frequency increases and at some frequency difference the pattern becomes stationary.

Figure 4 shows the region of similar frequencies as a plot of  $V_{th}$  versus  $\nu^{1/2}$ . The above-described temporal behavior of the diffraction pattern is evidently determined by the time required for the structure, which arises after the instability of the uniform distribution of the director, to intergrow and vanish.

3. The explanation of the observed characteristics of the behavior of the threshold values of the external electric field as a function of the relative frequency is based on the dynamics of the mesophase, which in our case depends on the behavior of the fast (charge) and slow (director) subsystems of the medium. When the conditions of applica-

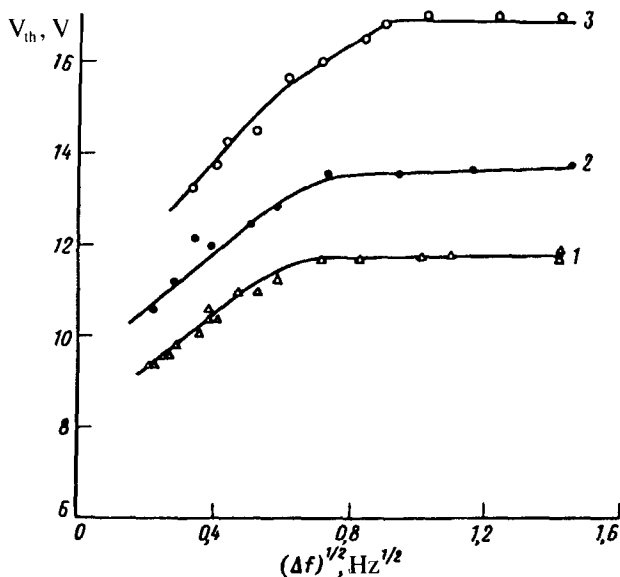


FIG. 4.  $V_{th}$  in the beat regime versus the frequency  $(\Delta f)^{1/2} = (f_1 - f_2)^{1/2}$  with fixed frequency  $f_2$ : curve 1—100 Hz; 2—200 Hz; 3—300 Hz.

bility are satisfied, it can be assumed that the dynamics of the liquid crystal is described by the well-known equations<sup>1-4</sup>

$$\dot{q} + \omega_c q + \sigma_H E \Psi = 0, \quad \dot{\Psi} + \omega_0 \Psi + \lambda E^2 \Psi + \mu E q = 0. \quad (1)$$

The first equation describes the dynamics of the charge  $q$  and the second equation describes the curvature of the director  $\Psi = \partial\theta/\partial z$ , where  $\theta$  is the angle between the director and the  $x$  axis, which is directed along the sample. A biharmonic electric field is applied perpendicular to the sample:  $E = E_0 \cos \omega_1 t + E_0 \cos \omega_2 t = 2E_0 \times \cos \omega t \cos \Delta\omega t$ ,  $\omega \equiv 1/2(\omega_1 + \omega_2)$ ,  $\Delta\omega \equiv 1/2(\omega_1 - \omega_2)$ . The parameters  $\omega_c$ ,  $\omega_0$ ,  $\sigma_H$ ,  $\lambda$ , and  $\mu$  have the same meaning as in Refs. 1-4.

The behavior of the medium depends on the ratio of the applied frequencies and the relaxation times of the charge and the director. To determine the character of the behavior of the mesophase, we introduce fast and slow variables:  $q = \bar{q} + \delta q$ ,  $\Psi = \bar{\Psi} + \delta\Psi$ , where  $\bar{q}$  and  $\bar{\Psi}$  describe the values of the charge and curvature averaged over a long segment of time, and  $\delta q$  and  $\delta\Psi$  are the fast changes in the separate subsystems. Substituting this representation into Eq. (1) and performing the corresponding averaging, we obtain the equations

$$\dot{\bar{q}} + \omega_c \bar{q} + \sigma_H \overline{E \delta \Psi} = 0, \quad \dot{\bar{\Psi}} + (\omega_0 + \lambda \overline{E^2}) \bar{\Psi} + \mu E \overline{\delta q} = 0. \quad (2)$$

Subtracting Eq. (2) from Eq. (1), we obtain the following system of equations for the fast variables:

$$\delta \dot{q} + \omega_c \delta q + \sigma_H E \overline{\delta \Psi} = 0, \quad \delta \dot{\Psi} + (\omega_0 + \lambda \overline{E^2}) \delta \Psi + \mu E \overline{\delta q} = 0. \quad (3)$$

In Eqs. (2) and (3) only the lowest harmonics of the frequency  $\omega$  are retained. The overbar on the separate terms indicates averaging over the corresponding times. Depending on the observed regimes, the averaging procedure and, correspondingly, the behavior of the medium will be different.

a) In the case where the frequency difference is large ( $\omega_1 \gg \omega_2$ ,  $\omega$ ,  $\Delta\omega$ ,  $\omega_1 \gg \omega_c, \omega_0$ ), the averaging must be performed over times such that  $\Delta\omega T \gg 1$ . The behavior of the mesophase can then be described by slow changes in the quantities  $\bar{\Psi}$  and  $\bar{q}$  over a time much longer than the averaging time. In solving the system (3), the total time dependence of  $E$  must be taken into account and the solutions for  $\delta q$  and  $\delta\Psi$  must be sought in the form

$$\begin{aligned} \begin{Bmatrix} \delta q \\ \delta\Psi \end{Bmatrix} = & \begin{Bmatrix} a_1 \\ b_1 \end{Bmatrix} \sin \omega t \sin \Delta\omega t + \begin{Bmatrix} a_2 \\ b_2 \end{Bmatrix} \sin \omega t \cos \Delta\omega t \\ & + \begin{Bmatrix} a_3 \\ b_3 \end{Bmatrix} \cos \omega t \sin \Delta\omega t + \begin{Bmatrix} a_4 \\ b_4 \end{Bmatrix} \cos \omega t \cos \Delta\omega t, \end{aligned} \quad (4)$$

where the top rows refer to  $\delta q$  and the bottom rows refer to  $\delta\Psi$ . Substituting expression (4) into the corresponding equations [Eqs. (3)] and equating the coefficients of the same combinations of transcendental functions, we obtain an algebraic system for determining the coefficients  $a$  and  $b$ . Having found the corresponding coefficients and having performed the averaging  $\overline{E\delta q} = 1/2E_0a_4$ ,  $\overline{E\delta\Psi} = 1/2E_0b_4$ ,  $\overline{E^2} = E_0^2$ , we obtain closed equations for  $\bar{\Psi}$  and  $\bar{q}$

$$\begin{aligned} \dot{\bar{\Psi}} + \left\{ \omega_d - \frac{E_0^2 \sigma_H \mu \omega_c (\omega^2 + \omega_c^2 + \Delta\omega^2)}{(\omega^2 + \omega_c^2 + \Delta\omega^2)^2 - 4\Delta\omega^2 \omega^2} \right\} \bar{\Psi} &= 0, \\ \dot{\bar{q}} + \left\{ \omega_c - \frac{E_0^2 \sigma_H \mu \omega_d (\omega^2 + \omega_d^2 + \Delta\omega^2)}{(\omega^2 + \omega_d^2 + \Delta\omega^2)^2 - 4\Delta\omega^2 \omega^2} \right\} \bar{q} &= 0, \end{aligned} \quad (5)$$

where  $\omega_d = \omega_0 + \lambda E_0^2$ . Equating to zero the damping rates of the solutions of system (5), we obtain a condition for finding the critical field for the appearance of instabilities. In the conduction regime, which is described by the first equation, the critical field is

$$E_c^2 = \frac{\omega_0}{\lambda} \frac{2(\omega_1^2 + \omega_c^2)(\omega_2^2 + \omega_c^2)}{\xi^2 \omega_c^2 (\omega_1^2 + \omega_2^2 + 2\omega_c^2) - 2(\omega_1^2 + \omega_c^2)(\omega_2^2 + \omega_c^2)}, \quad (6)$$

where  $\xi^2 = \mu\sigma_H/\omega_c$  has the same meaning as in Refs. 1-4. In the dielectric regime, where  $\omega_d = \lambda E_0^2$ , we obtain  $E_c^2 = 2\omega_2/\lambda(\xi^2 - 2)^{1/2}$ . It is evident from expression (6) that switching of the regimes occurs at the frequency

$$\omega_1^2 = \omega_k^2 \equiv \omega_c^2 \left\{ \frac{\xi^2(1 + \omega_2^2/\omega_c^2)}{2(1 + \omega_2^2/\omega_c^2) - \xi^2} - 1 \right\},$$

which in the two-frequency regime is not always satisfied. For example, for  $\xi^2 > 2(1 + \omega_2^2/\omega_c^2)$  switching of regimes does not occur. This was confirmed experimentally in the present work. Moreover, the theoretical dependence of the magnitude of the critical field on the frequencies  $\omega_1$  and  $\omega_2$ , as calculated from Eq. (6), agrees very well

with the experimental data. For  $\omega_1 \gg \omega_c > \omega_2$  the critical field no longer depends on the high frequency and saturates at the value  $E_c^2 = \omega_0^2 \cdot 2/\lambda (\xi^2 - 2)$ , which was also confirmed experimentally (Fig. 3). Admittedly, to obtain quantitative agreement between the experimental values of the critical field and the theoretical calculations, it must be assumed that the coefficient  $\xi^2$  depends on the lower frequency; this can be explained by the dispersion of the Leslie coefficients. It is well known that in this frequency range the Leslie coefficients can exhibit dispersion<sup>5</sup> and the sharp temperature dependence of  $\xi^2$ , observed experimentally, indicates that  $\xi^2$  is very sensitive to the viscosity, which can be expressed in terms of these coefficients.

b) We now consider the case in which the applied frequencies are close; specifically,  $\Delta\omega \ll \omega$ . In this case the dependence on the slow change of the parameters after averaging must be retained, for example,

$$\bar{E}^2 = \frac{1}{T} \int_0^T E(t) dt = 2E_0^2 \cos \Delta\omega t.$$

Determining  $\delta q$  and  $\delta\Psi$  from the system of equations (3) and substituting the results into Eq. (1), we obtain equations for  $\bar{\Psi}$  and  $\bar{q}$ . Since the experiment requires that the slow subsystem be observed, we present here only the equation for  $\bar{\Psi}$ :

$$\bar{\Psi} + \left\{ \omega_0 + \left( \lambda - \frac{\mu\sigma_H\omega_c}{\omega^2 + \omega_c^2} \right) E_0^2 + \left( \lambda - \frac{\mu\sigma_H\omega_c}{\omega^2 + \omega_c^2} \right) E_0^2 \cos 2\Delta\omega t \right\} \bar{\Psi} = 0, \quad (7)$$

whose solution is

$$\bar{\Psi} = \text{const} \cdot \exp \left\{ -\gamma t - \frac{\gamma}{2\Delta\omega} \sin 2\Delta\omega t \right\}, \quad (8)$$

where  $\gamma = \omega_0 + \left\{ \lambda - \frac{\mu\sigma_H\omega_c}{\omega^2 + \omega_c^2} \right\} E_0^2$ . The critical field in which the instability first appears is determined from the condition  $\gamma = 0$ . This field is

$$E_{0c}^2 = \frac{\omega_0}{\lambda} \frac{1 + \omega^2/\omega_c^2}{\xi^2 - (1 + \omega^2/\omega_c^2)}.$$

The experimentally observed "scintillation" of the new structure with the beat period  $2\pi/(\omega_1 - \omega_2)$  can thus be explained by the periodic behavior of the slope of the director in accordance with Eq. (8). The "intergrowth" of the structure can be explained on the basis of Eq. (8). The field  $\bar{E}$ , averaged over the frequency  $\omega$ , is a periodic function with the period  $T = \pi/\Delta\omega$ . If  $E_0 > E_{0c}$ , then the field  $\bar{E}$  can be greater than the critical field only for part of the period. Depending on this fraction and the magnitude of the field  $E_0$ , there may or may not be enough time for the structure to "intergrow" to the size recorded in the experiment (we have in mind the appearance of diffraction maxima). The field  $E_0$  for which the diffraction maxima first appeared was recorded in the experiment. This means that the quantity  $\bar{\Psi}$  was the same in each such measurement and corresponded to its maximum value over the period. Therefore, in our measurements we have

$$-\gamma T = -\frac{\gamma\pi}{2\Delta\omega} = \frac{\pi\omega_0}{2\Delta\omega} (E_0^2/E_{0c}^2 - 1), \quad (9)$$

we thus see that the observed values of the critical field are linear functions of  $(\Delta\omega)^{1/2}$ . The relation obtained above suggests a fast method for determining within only several periods the critical field for the appearance of Williams domains  $E_{0c}(\omega)$  with a fixed frequency  $\omega$ . For example, if  $E_0 = E_1$  for  $\Delta\omega = \Delta\omega_1$  and  $E_0 = E_2$  for  $\Delta\omega = \omega_2$ , we easily find that  $E_{0c}^2 = (E_2^2 - E_1^2 \Delta\omega_2 / \Delta\omega_1) / (1 - \Delta\omega_2 / \Delta\omega_1)$ . The experimental dependence of the critical field on the frequency difference (Fig. 4) agrees very well with the theoretical formula (9).

<sup>1</sup>L. M. Blinov, *Electro- and Magneto-Optics of Liquid Crystals* [in Russian], Nauka, Moscow, 1978.

<sup>2</sup>S. A. Pikin, *Structural Transformations in Liquid Crystals* [in Russian], Nauka, Moscow, 1978.

<sup>3</sup>P. G. de Gennes, *The Physics of Liquid Crystals*, Clarendon Press, Oxford, 1974; Mir, Moscow, 1977.

<sup>4</sup>S. Chandrasekhar, *Liquid Crystals*, Cambridge University Press, N. Y., 1993; Mir, Moscow, 1980.

<sup>5</sup>A. P. Kapustin, *Experimental Investigations of Liquid Crystals* [in Russian], Nauka, Moscow, 1978.

Translated by M. E. Alferieff